

Extremely-Metal Poor Stars in the Milky Way: A Second Generation Formed after Reionization

Michele Trenti and J. Michael Shull

*University of Colorado, CASA, Dept. of Astrophysical & Planetary Sciences, 389-UCB,
Boulder, CO 80309, USA*

trenti@colorado.edu, michael.shull@colorado.edu

ABSTRACT

Cosmological simulations of Population III star formation suggest an initial mass function (IMF) biased toward very massive stars ($M \gtrsim 100 M_{\odot}$) formed in minihalos at redshift $z \gtrsim 20$, when the cooling is driven by molecular hydrogen. However, this result conflicts with observations of extremely-metal poor (EMP) stars in the Milky Way halo, whose r-process elemental abundances appear to be incompatible with those expected from very massive Population III progenitors. We propose a new solution to the problem in which the IMF of second-generation stars formed at $z \gtrsim 10$, before reionization, is deficient in sub-solar mass stars, owing to the high cosmic microwave background temperature floor. The observed EMP stars are formed preferentially at $z \lesssim 10$ in pockets of gas enriched to metallicity $Z \gtrsim 10^{-3.5} Z_{\odot}$ by winds from Population II stars. Our cosmological simulations of dark matter halos like the Milky Way show that current samples of EMP stars can only constrain the IMF of late-time Population III stars, formed at $z \lesssim 13$ in halos with virial temperature $T_{\text{vir}} \sim 10^4$ K. This suggests that pair instability supernovae were not produced primarily by this population. To begin probing the IMF of Population III stars formed at higher redshift will require a large survey, with at least 500 and probably several thousand EMP stars of metallicities $Z \approx 10^{-3.5} Z_{\odot}$.

Subject headings: galaxies: high-redshift - Galaxy: evolution - intergalactic medium - stars: abundances - cosmology: theory - stars: formation

1. Introduction

According to simulations, the first stars in the Universe began forming 50–100 million years after the Big Bang (redshifts $z = 30 - 50$) in mini-halos with virial temperatures $T_{\text{vir}} = 10^3$ K (Tegmark et al. 1997; Yoshida et al. 2003; Naoz et al. 2006; Trenti & Stiavelli 2007). To fix the semantics of early stellar populations, we define Population II (stars and gas) as material enriched to metallicities $Z > Z_{\text{crit}} \approx 10^{-3.5} Z_{\odot}$, at which point the star-formation mode and initial mass function (IMF) are altered through radiative cooling by metals, which dominate that of molecular hydrogen. The equality of the dynamical time and cooling time in a collapsing gas cloud marks the transition from a typical fragmentation mass of $\sim 10^3 M_{\odot}$ to a lower mass $M \lesssim 10^2 M_{\odot}$, whose exact value depends on possible coupling with the Cosmic Microwave Background (CMB) temperature (Smith et al. 2009; see also Bromm & Loeb 2003, Omukai et al. 2005). Therefore we define Population III as pristine, high-redshift stars formed from gas at zero or near zero ($Z < Z_{\text{crit}}$) metallicity (Bromm et al. 2001; Bromm & Larson 2004; Santoro & Shull 2006; Smith et al. 2009).

Initially very rare (one star per Gpc^3 at $z \approx 50$), these early generations of stars form at rates that increase rapidly in number toward lower redshift until they are eventually suppressed by radiative and chemical feedback (see Trenti et al. 2009 and references therein). The numerical simulations further suggest that the first-generation (Population III) stars formed in isolation, with an IMF with characteristic scale $\sim 100 M_{\odot}$ consistent with the fragmentation mass derived from simple cooling models (see Abel et al. 2002; Bromm et al. 2003; Bromm & Larson 2004; Yoshida et al. 2006; O’Shea & Norman 2007, 2008). This characteristic mass is set primarily by the physics of hydrogen cooling, as these stars lack metals and dust. Molecular hydrogen (H_2) can only cool the gas down to ~ 200 K (Galli & Palla 1998), at which point the gas reaches a density $\sim 10^4 \text{ cm}^{-3}$ with corresponding Jeans mass $M_J \sim 10^3 M_{\odot}$ (Yoshida et al. 2006). High accretion rates onto the protostellar core (10^{-4} to $10^{-2} M_{\odot} \text{ yr}^{-1}$, see O’Shea & Norman 2007) suggest that their final mass is likely to be $\gtrsim 100 M_{\odot}$. Radiative feedback will eventually shut down the accretion (Tan & McKee 2004), but this phase has not yet been simulated self-consistently.

In the presence of a strong flux in the H_2 Lyman-Werner (LW) bands, with energies between 11.15–13.6 eV, the primary (H_2) coolant of minihalos is photo-dissociated (Lepp & Shull 1983; Haiman et al. 1997; Machacek et al. 2003). Under these conditions, the minimum halo mass required for cooling increases from $\sim 10^6 M_{\odot}$ up to $\sim 10^8 M_{\odot}$, reflecting a rise in virial temperature from $T_{\text{vir}} \sim 10^3$ K to $\sim 10^4$ K (Machacek et al. 2003; Greif & Bromm 2006). In these larger halos, small clusters of Population III stars can form. The mass of the gas at the halo center is typically larger than in the case of a minihalo collapse, so a few tens of Jeans masses might be present. Because these second-generation

stars form relatively late, at $z \lesssim 15$, some of them can be made out of reionized gas with correspondingly smaller masses ($\sim 40 M_{\odot}$, see Yoshida et al. 2006).

A direct detection of Population III stars will be extremely challenging, even with the next generation of telescopes and instruments. A $100 M_{\odot}$ Population III star has an observed magnitude $m_{AB} \gtrsim 38$ at $z > 6$, whereas the *James Webb Space Telescope* (JWST) is limited to $m_{AB} \sim 31$. Thus, JWST will only be able to observe such stars in the unlikely event they form in large clusters (Trenti et al. 2009). Supernovae from massive Population III stars are bright enough to be seen at essentially any redshift, but their observed rate is low. Therefore, a combination of deep multi-epoch imaging and large area coverage is needed (Weinmann & Lilly 2005; Trenti et al. 2009).

Given the limited options for direct investigations of the properties of metal-free stars, indirect studies are the next best strategy. Such observations have been carried out to constrain the IMF of Pop III stars by studying the properties of the most metal-poor stars in the local universe (Freeman & Bland-Hawthorn 2002; Beers & Christlieb 2005; Frebel et al. 2007), where remnants of the first Population III stars could be found (Trenti et al. 2008). The idea behind these “galactic archeology” campaigns is that stars with very low metallicities $Z \lesssim 10^{-3.5} Z_{\odot}$ (approximately the critical metallicity marking the transition from Pop III to Pop II) are most likely second-generation objects formed from gas enriched by only one previous generation of stars. If this first generation of stars is very massive ($M \gtrsim 100 M_{\odot}$), Heger et al. (2003) find that a significant fraction with initial masses of $140 - 260 M_{\odot}$ will explode as pair instability supernovae (PISN) and produce no r-process elements (Heger & Woosley 2002; Tumlinson et al. 2004). Surveys for extremely metal-poor stars in the Milky Way (MW) have found hundreds of stars with metallicity $Z \lesssim 10^{-3} Z_{\odot}$ (Beers & Christlieb 2005; Schörck et al. 2009), but so far none of those stars matches the nucleosynthetic pattern of PISN progenitors (Tumlinson 2006; Frebel et al. 2009). Based on this observational evidence, it has been proposed that the IMF of Population III stars is peaked at lower masses, $\sim 30 M_{\odot}$ (Tumlinson 2006). This is in conflict with the results from numerical simulations of Pop III star-formation, which suggest higher masses for metal-free stars.

Several past investigations studied the connection between observed metallicity distribution of Galactic metal-poor stars and Population III stars. For example, Karlsson et al. (2008) follow in detail the self-enrichment of a single $\sim 10^8 M_{\odot}$ halo and argue that second generation stars enriched by PISNe would reach a metallicity $[\text{Ca}/\text{H}] \sim -2.5$, higher than the cutoff used for current EMP searches. Hence, the lack of PISNe signatures in stars considered to be second generation could simply be a result of an observational bias. Karlsson et al. (2008) show that their results are insensitive to a redshift-independent change of the PopIII

star formation efficiency. However their work does not take into account the suppression of Population III star formation in minihalos due to LW feedback, which varies with redshift. Therefore the metallicity overshooting by PISNe could possibly be less severe. A different explanation has been suggested by Salvadori et al. (2007). They use an analytic merger-tree code aimed at reproducing the $z = 0$ Galactic metallicity distribution. As a result of fine tuning their free parameters to match the $z = 0$ observations, they find a negligible probability of observing second generation stars. The robustness of their conclusion is difficult to evaluate, especially because their model has an idealized treatment of metal outflows and assumes a one-zone instantaneous mixing of metals for the gas outside star-forming halos. In addition, Population III stars are only assumed to form in halos with $T_{\text{vir}} \geq 10^4 \text{ K}$, completely neglecting formation in minihalos cooled by H_2 . Similar conclusions to Salvadori et al. (2007) have also been reached by Komiya et al. (2007, 2009) who also use an analytical merger-tree code (with instantaneous mixing approximation) and without taking into account the effects of radiative feedback on Population III star formation.

Both of these physical effects are examined in this paper, with the goal of quantifying the IGM enrichment by Population III stars and predicting the expected fraction of EMP stars with PISNe signatures. The context of our study takes into account the complex interplay of radiative and chemical feedback during the reionization epoch. We employ high-resolution cosmological simulations of structure formation, both for an average region of the Universe (in a comoving volume of 10^3 Mpc^3) and for three dark-matter halos similar in mass to the Milky Way. We post-process these simulations by taking into account additional physical processes that regulate star formation, beyond those considered in past investigations such as Tumlinson (2006); Salvadori et al. (2007); Komiya et al. (2007, 2009); Karlsson et al. (2008). These processes include: (1) radiative feedback on the cooling of metal-free minihalos; (2) spatial distribution of metal outflows from protogalaxies, missing in investigations based on analytical merger-tree codes; and (3) impact of the cosmic microwave background (CMB) temperature on the typical mass of Population II stars formed at high-redshift (Clarke & Bromm 2003; Tumlinson 2007; Smith et al. 2009).

This paper is organized as follows. In Section 2 we introduce our model and discuss the transition from Population III to Population II star formation and investigate its consequences for the chemical enrichment of second-generation gas in Section 3. Section 3 is based on analytical modeling and cosmological simulations representative of an average region of the high-redshift Universe. In Section 4 we present results from three constrained-realization simulations of halos like the Milky Way, and we discuss the differences with the averaged results obtained for a random region of the Universe. Section 5 concludes with a discussion of Milky Way EMP surveys needed to probe the metallicity distributions and set limits on PISN progenitors at $z \leq 10$.

2. Transition from Population III to Population II

In this analysis, we adopt the star formation model described in Trenti & Stiavelli (2009) and Trenti et al. (2009). We consider the halo dynamics in a dark-matter scenario, based either on Press-Schechter modeling plus an analytical expression for self-enrichment probability (see Trenti & Stiavelli 2007) or on detailed halo-merger histories derived from cosmological simulations (Trenti et al. 2009). Dark matter halos are populated according to an analytical cooling model that takes into account radiative feedback in the LW bands of H_2 , self-enrichment, and wind enrichment, the latter limited to the star formation histories from numerical simulations. A single, massive, Pop III star is assumed to form in halos with $Z < Z_{\text{crit}}$ and $10^3\text{K} \leq T_{\text{vir}} \leq 10^4\text{K}$. The precise value of T_{vir} required for Pop III formation depends on redshift and is derived considering the negative (H_2 LW-band) feedback self-consistently determined from the star formation rate. Pop III stars are assumed to end their life as a Pair Instability Supernova (Heger & Woosley 2002), while a constant fraction of gas (typically $f_* \approx 10^{-2}$) is converted into stars for metal-enriched halos with a minimum $T_{\text{vir}} \geq 10^4$ K. Multiple Pop III stars are optionally allowed to form in the same halo when $\text{Ly}\alpha$ cooling is possible, in metal-free halos with $T_{\text{vir}} \geq 10^4$ K.

Because of the large amount of metals (50–100 M_{\odot}) released by a PISN explosion (Heger & Woosley 2002; Heger et al. 2003; Gal-Yam et al. 2009), a single Population III progenitor is sufficient to enrich a descendant halo with $T_{\text{vir}} \sim 10^4$ K to Z_{crit} . The violent relaxation (Lynden-Bell 1967) associated with the virialization of the descendant halo provides efficient mixing of the metals, initially concentrated in a ~ 1 kpc region around the site of explosion (Bromm et al. 2003). However, the metal outflow from a PISN is confined to the region occupied by a $T_{\text{vir}} \lesssim 10^4$ K halo (Bromm et al. 2003). Hence, Population III stars formed in isolation only contribute to genetic enrichment of their descendant halos and are not expected to pollute nearby halos. Metal outflows are instead expected from the Population II galaxies in halos with $T_{\text{vir}} \gtrsim 10^4$ K. These outflows are estimated to travel at average velocities of $40 - 100 \text{ km s}^{-1}$ and can enrich a region of radius $\sim 100 h^{-1}$ kpc (Madau et al. 2001; Furlanetto & Loeb 2003; Tumlinson et al. 2004). We assume conservatively a star-formation efficiency $f_* = 0.01$ and a metal yield of $y_m = 1/40$, derived for a local $z = 0$ IMF, hence likely an underestimate at $z \gtrsim 6$ given the effect of the CMB temperature. We find that an outflow originating from a $M = 10^8 M_{\odot}$ halo can enrich to $Z \sim Z_{\text{crit}}$ a fully virialized $10^8 M_{\odot}$ halo within $d \lesssim 33 h^{-1}$ kpc or a region containing the same mass in the process of virialization (with overdensity $\Delta\rho/\langle\rho\rangle = 2$) out to $d \lesssim 150 h^{-1}$ kpc. To model wind enrichment from the cosmological simulations, we therefore save snapshots with high-frequency ($\Delta z = 0.125$ at $z \leq 10$ and $\Delta z = 0.25$ at $10 \leq z \leq 15$) and track during post-processing the expansion of metal outflows originating from Population II halos. We assume that a halo with $T_{\text{vir}} \gtrsim 10^4$ K is enriched to $Z \gtrsim Z_{\text{crit}}$ (if not already above this

threshold) once it is reached by the front of a metal outflow.

Therefore, in our model, the gas is either pristine or above the critical metallicity. For a lower value of Z_{crit} , possible in presence of dust (Schneider et al. 2006), this assumption would be even better justified. Our standard analysis is carried out for $v_{\text{wind}} = 60 \text{ km s}^{-1}$, but we also investigate $v_{\text{wind}} = 40 \text{ km s}^{-1}$ and $v_{\text{wind}} = 100 \text{ km s}^{-1}$. Note that in our treatment of metal enrichment and star formation, metal-free halos with $T_{\text{vir}} \geq 10^4 \text{ K}$ are assumed to form a first generation of massive metal-free stars, immediately followed by a second generation of stars with $Z \gtrsim Z_{\text{crit}}$. This implies that we are effectively setting the lifetime of a Population III star to zero and assuming instantaneous recycling for genetic enrichment in $T_{\text{vir}} \geq 10^4 \text{ K}$ halos. In this approximation, we neglect the small fraction of halos that are quickly reached by a metal outflow, within a few Myr after hosting a burst of Population III star formation. Because winds propagate for $\gtrsim 100 \text{ Myr}$ before reaching a metal-free halo, accounting for the lifetime of a massive Population III star would be equivalent to increasing v_{wind} by $\lesssim 5\%$. This has a minimal impact in our model given the larger uncertainty on other parameters.

We now summarize the main results of our model (Trenti et al. 2009), crucial to interpret the observed enrichment pattern in Galactic extremely metal-poor stars:

1. Population III star formation in minihalos cooled by H_2 starts at very high redshift ($z \gtrsim 45$) for a comoving volume comparable to that of a MW-like halo. Radiative feedback begins quenching this mode of star-formation at $z \sim 35$ and completely suppresses it by $z \sim 15$. For a given star formation rate, the flux in the LW bands is almost IMF and metallicity independent, a very marked difference compared to the ionizing flux, which increases significantly for a top-heavy IMF and for extremely low or zero metallicity (Schaerer 2003, Table 4).
2. The metal-enriched star formation rate becomes higher than the metal-free rate at $z \sim 25$ and continues to increase almost exponentially until $z \sim 10$. At $z \sim 20$, Pop II stars are already the dominant star-formation mode and implies that metal-free stars are probably minor players in reionizing the Universe. At $z \lesssim 25$, LW photons are primarily produced by metal enriched stars.
3. Population III star-formation continues to be possible at $z < 15$ at a comoving rate $\sim 10^{-6} \text{ M}_{\odot} \text{ yr}^{-1} \text{ Mpc}^{-3}$ in larger halos with $T_{\text{vir}} \gtrsim 10^4 \text{ K}$, insensitive to the LW photo-dissociating background. Winds from nearby Pop II halos enrich all the IGM by $z \sim 4$, progressively reducing the Pop III star formation rate, beginning at $z \sim 10$.

3. Second-generation Star Formation in average regions

The complex star-formation history derived in Trenti et al. (2009) raises two questions in the context of the observed chemical abundances of EMP stars: First, what are the expected chemical progenitors of EMP stars? Are they Pop III stars in minihalos, Pop III stars in the larger $T_{\text{vir}} \sim 10^4$ K halos (via self-enrichment), or Pop II stars (via winds)? Second, over which redshift range did the *currently observable* EMP stars form?

We first address these questions for an average region of the Universe, using the $N = 1024^3$ dark matter particle cosmological simulation of Trenti et al. (2009), with a comoving volume $V = 10^3$ Mpc³, a single-particle mass $3.4 \times 10^4 M_{\odot}$, and a force resolution of $0.16 h^{-1}$ kpc. We adopt a cosmology based on the fifth-year WMAP data (Komatsu et al. 2009): $\Omega_{\Lambda} = 0.72$, $\Omega_m = 0.28$, $\Omega_b = 0.0462$, $H_0 = 70$ km s⁻¹ Mpc⁻¹, and $\sigma_8 = 0.817$. The initial conditions have been generated at $z = 199$ with a code based on the Grafic algorithm (Bertschinger 2001) using a Λ CDM transfer function computed via the fit by Eisenstein & Hu (1999) with spectral index $n_s = 0.96$. Halos are identified with a friend-of-friend halo finder (Davis et al. 1985) using a linking length equal to 0.2 of the mean particle separation. A halo merger tree is constructed from the particle IDs to track metal enrichment derived from progenitor halos.

We define “second-generation gas” as gas at $Z > Z_{\text{crit}}$, residing in a $T_{\text{vir}} \geq 10^4$ K halo with no progenitor that experienced Population II star formation in a previous snapshot. Next, we must distinguish between “second-generation gas” enriched by Pop II or Pop III stars. The earliest gas was enriched by Pop III stars in dark matter halos with $T_{\text{vir}} \geq 10^4$ K. During the halo merging history, such halos had at least one progenitor halo that hosted a Pop III star, but no progenitors with Pop II stars. In contrast, second-generation gas enriched by Pop II stars is defined as gas in a dark matter halo with $T_{\text{vir}} \geq 10^4$ K whose progenitor halos had no star formation and were chemically enriched by winds originating in a nearby halo¹.

Figure 1 shows that most (about 60%) of the second-generation gas is enriched by Pop II winds. In addition, Pop III stars in minihalos (formed at $z \gtrsim 14$) only contribute to a small fraction (about 10%) of second-generation enrichment; this gas is highlighted as the shaded area in Fig. 1. This surprising result can be understood from the star-formation rate history plotted in Fig. 1 of Trenti & Stiavelli (2009). The Pop III star formation rate per unit time remains relatively constant from $z \sim 40$ to $z \sim 10$, so that most of the stars are formed

¹The majority of halos with $T_{\text{vir}} > 10^4$ K in the simulation box have metal-enriched halos as progenitors and thus host at least third-generation stars.

at the lower end of the interval. (Note that cosmological time scales as $t \propto (1+z)^{-3/2}$). As time passes, metal-enriched winds from Pop II galaxies fill progressively more volume, enriching pockets of low-metallicity gas that never underwent self-enrichment because the strong radiative (LW) background suppressed H_2 cooling (see also Fig. 4 in Trenti et al. 2009). Figure 1 was obtained for $v_{\text{wind}} = 60 \text{ km s}^{-1}$. Faster winds increase the fraction of the gas enriched by Pop II stars, while slower winds favor a higher fraction of Pop III IGM enrichment (see Fig. 5 in Trenti et al. 2009).

To translate the fraction of second-generation gas enriched by Pop III stars into a prediction for EMP star surveys, we need to address the second question raised above, namely when did *currently observable* EMP stars form? These stars can be observed only if they are bright nearby main-sequence stars or lie along the giant branch. Given that second-generation stars are quite old (they formed at $z \gtrsim 4$ according to Fig. 1), we can observe them only if their initial mass was $M \lesssim 0.9 M_{\odot}$. For the present-day IMF, most of the stars formed lie below this cut-off. However, this was not necessarily true at earlier times, because coupling with the CMB radiation prevents the gas to cool below T_{CMB} (Clarke & Bromm 2003; Tumlinson 2007; Smith et al. 2009)². In fact, the fragmentation scale of protostellar clouds is probably set by the Jeans mass (Larson 2005; Tumlinson 2007), which depends on the temperature T_{min} and density ρ of the gas:

$$M_J = \left(\frac{\pi k T_{\text{min}}}{2 m_H G} \right)^{3/2} \rho^{-1/2}. \quad (1)$$

By adopting a power-law equation of state, Tumlinson (2007) expresses the typical stellar mass in the IMF as a function of redshift:

$$M_C = M_{\text{norm}} \left\{ \frac{\max[2.73(1+z), 8]}{10 \text{ K}} \right\}^{\alpha}, \quad (2)$$

where α depends on the equation of state, with an expected range $1.7 \leq \alpha \leq 3.35$, and the normalization M_{norm} is defined as:

$$M_{\text{norm}} = \frac{0.5 M_{\odot}}{0.8^{\alpha}}, \quad (3)$$

based on a typical temperature of 8 K and a typical mass of $0.5 M_{\odot}$ observed in the local Universe (Kroupa 2002). Equation 2 can then be used to define the IMF, parameterized in log-normal form (Eq. 4 in Tumlinson 2007):

$$\ln \left(\frac{dN}{d \ln M} \right) = A - \frac{1}{2\sigma^2} \left[\ln \left(\frac{M}{M_C} \right) \right]^2, \quad (4)$$

²Note that the coupling is relevant only for gas at $Z \gtrsim Z_{\text{crit}}$, because Population III halos cannot easily reach temperatures below $T \sim 200 \text{ K}$, already higher than T_{CMB} at $z < 70$.

where A is a normalization constant and σ is a free parameter of order unity that controls the width of the distribution.

From Eq. 2 and Eq. 4 we can compute the number of second-generation stars (defined as stars formed out of “second-generation” gas) still observable today, with $M \leq 0.9 M_{\odot}$. If we are interested only in the relative fraction of EMP enriched by Pop III vs. those enriched by Pop II, our result does not depend on the EMP-star formation efficiency, as long as we assume a constant efficiency per unit mass in transforming gas to stars. Figure 2 shows this fraction, defined as

$$\epsilon = N_{\text{PopIII-enriched}} / (N_{\text{PopII-enriched}} + N_{\text{PopIII-enriched}}) \quad (5)$$

as a function of (σ, α) . Here, σ is the IMF mass width, and α is the exponent that regulates the typical stellar mass as a function of the CMB temperature (Eq. 2). Even for a very broad IMF ($\sigma = 1.4$) and a shallow redshift evolution of the typical stellar mass ($\alpha = 1.7$), only up to $\sim 25\%$ of observable EMP stars are formed out of Pop III-enriched gas. For intermediate values of the IMF parameters, we obtain $\epsilon \sim 0.15$, while an extremely narrow IMF reduces ϵ to ~ 0.06 . These numbers imply that a significant sample of EMP stars with metallicity $Z \sim 10^{-3.5} Z_{\odot}$ is required to rule out the null hypothesis that Pop III stars are very massive and preferentially explode as PISN (see Table 1). For a Poisson distribution, $P(k) = N_{exp}^k \exp(-N_{exp}) / k!$, with expected value N_{exp} , the probability of zero events is $P(0) = \exp(-N_{exp})$. Thus, the minimum second-generation sample size to rule out that a fraction η of Population III stars exploded as PISNe at a confidence level ξ ($0 < \xi < 1$) is:

$$N_{min} = \frac{-\log(1 - \xi)}{\epsilon(\alpha, \sigma)\eta}. \quad (6)$$

For example, to rule out at 99% of confidence level ($\xi = 0.99$) that 50% of Pop III stars explode as PISN, we need 41–135 second-generation stars, depending on the parameters assumed for the IMF of the EMP stars.

With the same approach, we can estimate the size of the sample required to investigate the IMF of Pop III stars in minihalos at $z \gtrsim 15$. The fraction of early-time Pop III-enriched second-generation stars for this case is shown in Fig. 3. We note the limited amount of gas enriched by this sub-class of Pop III stars (see Fig. 1) as well as the increase of the typical EMP stellar mass as a function of redshift (see Eq. 2). It is highly unlikely to observe one of these second-generation stars today. In fact, we find $\epsilon \leq 0.02$ over the entire EMP-IMF parameter space. The main controlling parameter is σ , the IMF width. Under the most optimistic assumptions for σ and α in Table 1, about 1775 second-generation stars are required to reject the hypothesis of 50% PISN from metal-free stars in minihalos at 99% CL. If the EMP-IMF is narrower, a sample size above 10^4 sources is required. As we discuss

in Trenti et al. (2009), the formation rate of minihalos, as measured in our cosmological simulation, might be slightly underestimated owing to resolution issues. If this is the case, the size of the second-generation star sample is reduced accordingly. Conservatively assuming a factor-of-two higher Pop III formation rate in minihalos implies a sample size $\gtrsim 900$ second-generation stars.

4. Second-Generation Star Formation in Milky-Way like halos

The star formation model in Section 3 describes an average region of the Universe at $z \geq 4$. Instead, the MW progenitors lived in a region with an above-average halo formation rate because of the presence of the large-scale overdensity that created the MW and the Local Group at $z \lesssim 1$. As a result, the star-formation history of the region is enhanced and tends to be shifted earlier in time compared with a typical region of the Universe. This introduces two competing factors that can affect the expected fraction of observable second generation stars enriched by Pop III stars. First, metal winds have had less time to reach nearby halos, so we expect a larger fraction of second generation gas enriched by Pop III stars. This effect is balanced by the higher CMB temperature floor present at earlier times, which makes it more difficult for stars formed out of this gas to have sub-solar masses and thus be observable today.

To quantify this scenario and to obtain a detailed prediction to compare with EMP surveys in the MW, we consider a new set of cosmological simulations, with the same setup of the one considered in Section 3, except for the initial conditions. Here, we use the Gfric package (Bertschinger 2001) and set the initial conditions to host a MW-like halo at $z = 0$ at the center of the simulation box. Because of the prohibitive computational time needed to evolve to $z = 0$ a $V = 10^3 \text{ Mpc}^3$ volume with $N = 1024^3$ particles, we first run a low-resolution ($N_{lr} = 128^3$) version of the simulation box to $z = 0$ to measure directly the central halo mass realized in the initial conditions. We consider three different realizations of central halos to explore a range of masses and formation histories: $M_1 = 3.15 \times 10^{12} M_\odot$ (corresponding to 172,981 low-resolution particles), $M_2 = 2.60 \times 10^{12} M_\odot$, and $M_3 = 1.59 \times 10^{12} M_\odot$. From $z = 1$ to $z = 0$, halo 1 acquires 45% of its mass, similar to halo 3 (42%), while halo 2 experiences a major merger and acquires 59% of its mass. A projection of the halos at $z = 0$ (region size $\sim 1 \text{ Mpc}^2$) from the low-resolution run is shown in the upper left panel of Figs. 4-6.

We then create the final full resolution ($N = 1024^3$) box by keeping the same large-scale structure of the low-resolution version using the Hoffman & Ribak (1991) method. Each low-resolution particle is thus associated with $n_c = 1024^3/128^3 = 512$ “child” particles in

the high-resolution run. Based on the initial positions, we map the IDs of the particles in the central halo of the low resolution realization into the set of high-resolution particle IDs expected to be part of this central halo. We tested this method extensively with a series of constrained simulations at different resolution and found that, for a halo resolved with $\sim 10^5$ low-resolution particles, the mass (and hence halo membership) is accurate at the $\gtrsim 97\%$ level (Trenti et al., submitted). The setup we choose is similar in terms of mass resolution and number of particles to that adopted by Tumlinson (2009)³, with the only difference being that Tumlinson (2009) binned particle positions and velocities to reduce the resolution and complete the run from $z = 4$ to $z = 0$ rather than using the Hoffman & Ribak (1991) method.

The post-processing analysis is the same discussed in Section 3, with the difference that the results on second-generation gas are given only for halos that are progenitors of the central $z = 0$ MW-like halo. The comoving volume considered for normalization is that occupied at $z = 199$ by the particles that end up at $z = 0$ in the central halo. The number of particles in this volume range from $> 88 \times 10^6$ for halo 1 to $> 44 \times 10^6$ for halo 3.

Figures 4-6 summarize the results for the different halos. The formation rate per unit redshift per unit volume of second generation gas is shown in the upper right panel of the figures as solid lines and compared to the box-averaged formation rate (dotted lines). As expected, the regions where the progenitors of MW-like halos live have an enhanced halo formation rate and higher clustering than an average region of the Universe. As a consequence, metal enrichment by Population III stars is more efficient (by $\gtrsim 50\%$) at $z \gtrsim 10$. This is consistent with a very simple estimate based on linear theory: the region hosting a MW-like halo at $z = 0$ has an average overdensity $\Delta\rho/\langle\rho\rangle \sim 0.14$ at $z = 15$. This in turn implies that the comoving number density of halos with $M = 1.4 \times 10^7 M_\odot$ (hosting Population III stars at $z = 15$, see Trenti et al. 2009), derived from the Sheth & Tormen (1999) mass function, is enhanced from $\sim 5.6 \text{ Mpc}^{-3}$ to $\sim 8.9 \text{ Mpc}^{-3}$.

Because of the higher clustering, winds are also more efficient at polluting nearby, non self-enriched halos. At $z \lesssim 10$ the formation rate of Population III enriched gas becomes comparable to the average in the Universe. The enhanced formation rate of $T_{\text{vir}} \sim 10^4 \text{ K}$ halos is balanced by a higher fraction of such halos reached by metal outflows. Consequently, the number density of wind-enriched halos also increases compared to the box average. By $z \sim 6$ the number density of wind-enriched halos has returned to values similar to those of an average region of the universe. This can be again understood in terms of linear theory. $T_{\text{vir}} \sim 10^4$ halos are common at $z \lesssim 6$: based on their rarity, measured in terms of the Press-

³The preprint was posted on arxiv while this paper was being revised

Schechter variable $\nu = \delta_c^2 / \sigma_{DM}^2(M)$, these halos have $\nu \sim 1.38$ on average in the Universe. The $z = 5$ overdensity associated with a MW-like halo at $z = 0$ only decreases this rarity to $\nu \sim 1.14$, and the number density of such overdensities is comparable: $\sim 8.7 \text{ Mpc}^{-3}$ on average versus $\sim 9.4 \text{ Mpc}^{-3}$ for the MW-like region. The three different halos we consider have all a similar enrichment history at $z \geq 4$.

The predictions for the fraction ϵ of second-generation stars enriched by Population III metals is shown in the bottom panels of Figures 4-6 considering all Population III stars (left panels — equivalent to Figure 2) and only Population III in minihalos (right panel — equivalent to Figure 3). Given the two competing effects discussed above (higher halo formation rate and higher efficiency of wind pollution), the contour lines of $\epsilon(\sigma, \alpha)$ are similar to those of the box-average. There is a moderate tendency to lower values for ϵ , implying that the fraction of second-generation stars enriched only by Population III metals can be observed today is smaller than the one estimated for the average of the Universe. Table 1 contains the minimum number of stars required to rule out a 50% PISNe fraction in Population III stars for MW halo 1 based on Equation 6. Minimum sample sizes for halo 2 and halo 3 are similar. Depending on the IMF parameters, (α, σ) , the sample sizes for all Pop III enrichment range from a factor of a few difference with the box-average (at low σ) to almost equal to the box average (for high σ and low α). For enrichment by minihalos-Pop III in MW-like progenitors, the required sample sizes are about two times smaller than those derived in a random region (because of the factor two increase in the gas enriched by these stars compared to an average region of the Universe).

Our main conclusion, namely the very small fraction of second-generation stars enriched by Population III stars observable today, is similar to that found by Salvadori et al. (2007), although their modeling assumptions are different from ours. In particular, the instantaneous, single-zone recycling of metals implies a sharp cut-off of Population III formation, while in our model we find a long tail of metal-free star formation in halos with lower than average bias (see Fig. 3 in Trenti et al. 2009).

Figure 7 explores the impact of v_{wind} on the results from our model for halo 1. The outflow velocity is the key parameter controlling the relative fraction of Population III to Population II enriched gas. In the absence of winds, only self-enrichment is possible, hence all second-generation gas would be enriched by Population III metals. On the other hand, faster propagation of metal outflows suppresses low-redshift Population III formation. For example, $v_{wind} = 100 \text{ km s}^{-1}$ reduces by $\gtrsim 75\%$ the Population III star formation at $z \lesssim 8$ compared to the standard $v_{wind} = 60 \text{ km s}^{-1}$. Slower outflows, $v_{wind} = 40 \text{ km s}^{-1}$, increase the Population III star formation at low redshift by up to a factor two. This is reflected in the formation rate of second generation gas, shown in the upper panels of Figure. 7. The

lower panels contain the $\epsilon(\sigma, \alpha)$ contour lines for these models. Naturally, the fraction of observable second-generation stars increases for lower wind speed, but not dramatically. For example, $\epsilon \leq 0.23$ in the standard model, $\epsilon \leq 0.41$ for $v_{wind} = 40 \text{ km s}^{-1}$, and $\epsilon \leq 0.10$ for $v_{wind} = 100 \text{ km s}^{-1}$.

5. Conclusions and Discussion

In this paper, we propose a novel solution to the conflict between the extremely top-heavy Pop III IMF predicted from cosmological hydrodynamic simulations and the lack of PISN signatures in the metal abundances of EMP stars observed in the Milky Way halo. Compared to past studies with a similar goal, our model takes into account additional physical ingredients relevant for star formation and chemical enrichment during the reionization epoch. The most important addition is the inclusion of radiative feedback in the UV Lyman-Werner bands of H_2 , bands, which quenches Population III star formation in minihalos and increases the minimum halo mass required for cooling to $T_{\text{vir}} \sim 10^4 \text{ K}$ by $z \sim 15$ (see Trenti & Stiavelli 2009). Without this increase, we would have obtained a significantly higher self-enrichment efficiency and reduced the importance of metal outflows for enriching second-generation gas. We also base our analysis on high-resolution N-body simulations capable of resolving star forming minihalos, both in a 10^3 Mpc^3 (comoving) cosmological volume, as well as in three regions hosting a $z = 0$ halo similar in mass to that of the MW. These simulations allow us to quantify metal outflows from proto-galaxies, improving the instantaneous one-zone assumption in Salvadori et al. (2007), based on Press-Schechter merger trees, as well as the work of Karlsson et al. (2008), focused on self-enrichment of a single $10^8 M_{\odot}$ halo. A third novel key ingredient is the inclusion of the cosmic microwave background (CMB) coupling with cooling gas. This introduces a floor in the cooling of metal enriched halos and affects their initial stellar mass function (Clarke & Bromm 2003). This effect was also not modeled in Salvadori et al. (2007) or Karlsson et al. (2008).

With our assumptions, we have shown that observations and numerical simulations can be consistent. In fact, we find that the majority of observable EMP stars with $Z \sim 10^{-3.5} Z_{\odot}$ were probably formed out of gas enriched to this critical metallicity by Pop II winds at $z \lesssim 10$. Pop III stars formed in minihalos cooled by H_2 enrich only a small fraction, $\epsilon \sim 10^{-4}$ to 10^{-2} , of the gas that ends up in EMP stars with $M \leq 0.9 M_{\odot}$. The fraction of observable second-generation stars formed in regions enriched by late-time Pop III stars is even higher, ranging from 6% to 25%, depending on the details of the modeling, in particular the IMF width of the EMP stars.

The minimum sample sizes reported in Table 1 can be compared with the metallicity

distribution of EMP stars based on Galactic surveys such as the Hamburg/ESO survey (Christlieb et al. 2008) and the SDSS/SEGUE survey (Ivezić et al. 2008) that have identified several hundred metal-poor stars with $[\text{Fe}/\text{H}] < -3.0$ (Schörck et al. 2009). These surveys show a sharp cutoff at $[\text{Fe}/\text{H}] < -3.6$, consistent with the theoretical expectation of $Z_{crit} \sim 10^{-3.5} Z_{\odot}$. To infer the Pop III IMF, we should ideally use only those EMP stars close to the critical metallicity for the transition to Pop II star formation. This would help to avoid contamination in the sample by third-or-higher generation stars formed in gas with a lower than average enrichment history. This issue is especially important if the lack of PISN chemical signatures in second-generation stars is used to argue against very massive Pop III star progenitors. A single PISN producing $10 M_{\odot}$ of iron can pollute $10^7 M_{\odot}$ of gas (the typical content of a $T_{vir} \sim 10^4$ K halo) to a metallicity $[\text{Fe}/\text{H}] \sim -3.2$, assuming homogeneous mixing. This is a level slightly higher than the observed cut-off at $[\text{Fe}/\text{H}] \sim -3.6$, suggesting that it would be important to improve instantaneous one-zone metal enrichment assumptions. Except for this caveat, we thus suggest that the analysis should be confined to a sample of EMP stars with $[\text{Fe}/\text{H}] \lesssim -3.4$ to identify second-generation stars. The HES survey has 14 such stars (Schörck et al. 2009). A few other EMP with $[\text{Fe}/\text{H}] \lesssim -3.5$ also have published metallicities (see Beers & Christlieb 2005 for a recent review). Based on this sample size, we would have expected on average a few of these stars to show PISN signatures in their abundances if a significant fraction of late-time Pop III stars were in the $140\text{-}260 M_{\odot}$ range. A larger sample of EMP stars, likely available in the near future with extensions and/or follow-ups of the SEGUE and HES surveys, will be able to set stronger limits on the fraction of PISN originating at $z \lesssim 10$. Investigating the shape of the IMF for Pop III stars in minihalos would require an increase of about two orders of magnitude in the current sample of EMP stars.

Since the majority of Pop III numerical investigations have focused on Pop III stars in minihalos, there is no inconsistency with the observed abundances of EMP stars. The sample size used to search for PISN signatures is simply too small. The current EMP sample is now approaching a size that can yield solid constraints on the IMF of late-time Pop III stars (see Table 1). The absence of PISN signatures is still lacking a significant confidence level, but it is consistent with the predictions for Pop III star formation in (partially) reionized gas. It points toward a typical IMF mass of $\sim 30 M_{\odot}$ (Yoshida et al. 2006).

Our scenario for the formation of second-generation stars is also consistent with the observed distribution of the $[\text{Mg}/\text{H}]$ ratio for EMP stars (see Fig. 1 in Frebel et al. 2009). Magnesium abundances below the minimum level predicted by PISN nucleosynthesis, $[\text{Mg}/\text{H}] \lesssim -3.2$ (see Heger & Woosley 2002; Frebel et al. 2009) are naturally expected if the enrichment of second-generation stars with $M \leq 140 M_{\odot}$ is driven by Pop II winds and/or by Pop III stars formed in (partially) reionized gas.

From our Figures 4-6, illustrating the chemical enrichment of MW-like halos, we see that the comoving star formation rate per unit redshift averages several times $10^7 M_\odot \text{Mpc}^{-3}$ over a redshift interval $\Delta z \approx 6$. Thus, in a comoving volume of 20Mpc^3 , approximately equivalent to the region that collapses into a MW-like halo, we estimate that $\sim 2.7 \times 10^9 M_\odot$ of second-generation gas was available to form stars. This is $\sim 2\%$ of the total baryonic mass of the Milky Way today. We expect that several thousand second-generation EMP stars could be observable today. For example, adopting a rather inefficient star formation efficiency of 0.1% and assuming that only 10^{-2} of the second-generation stars had an initial mass below $0.9 M_\odot$, we still expect a total of 2×10^4 EMP stars with $[\text{Fe}/\text{H}] \sim -3.5$ in the MW halo.

Finally, we have shown that the transition from Population III to Population II star formation that occurred at $z \gtrsim 4$ is not too different in the region that collapses at $z = 0$ in a MW-like halo compared to the average in the Universe (Figures 4-6). At $z \gtrsim 10$, the Population III star formation rate, and its associated chemical enrichment of second generation gas are about a factor two higher compared to the box-average. At $z = 10$, metal outflows from proto-galaxies are also more efficient, but by less than about a factor two. However, by $z \lesssim 6$, the formation rate of $10^8 M_\odot$ halos has returned to the average value in the Universe. Our findings demonstrate that constrained realizations of MW-like halos are not necessarily required to investigate the first steps in the build-up of our own Galaxy.

We thank Britton Smith and Massimo Stiavelli for useful comments and discussions. We acknowledge support from the University of Colorado Astrophysical Theory Program through grants from NASA (NNX07AG77G) and NSF (AST07-07474).

REFERENCES

- Abel, T., Bryan, G. L., & Norman, M. L. 2002, *Science*, 295, 93
- Beers, T. C. & Christlieb, N. 2005, *ARA&A*, 43, 531
- Bertschinger, E. 2001, *ApJS*, 137, 1
- Bromm, V., Ferrara, A., Coppi, P. S., & Larson, R. B. 2001, *MNRAS*, 328, 969
- Bromm, V. & Larson, R. B. 2004, *ARA&A*, 42, 79
- Bromm, V. & Loeb, A. 2003, *Nature*, 425, 812
- Bromm, V., Yoshida, N., & Hernquist, L. 2003, *ApJ*, 596, L135
- Christlieb, N., Schörck, T., Frebel, A., Beers, T. C., Wisotzki, L., & Reimers, D. 2008, *A&A*, 484, 721
- Clarke, C. J. & Bromm, V. 2003, *MNRAS*, 343, 1224
- Davis, M., Efstathiou, G., Frenk, C. S., & White, S. D. M. 1985, *ApJ*, 292, 371
- Eisenstein, D. J. & Hu, W. 1999, *ApJ*, 511, 5
- Frebel, A., Johnson, J. L., & Bromm, V. 2007, *MNRAS*, 380, L40
- . 2009, *MNRAS*, 392, L50
- Freeman, K. & Bland-Hawthorn, J. 2002, *ARA&A*, 40, 487
- Furlanetto, S. R. & Loeb, A. 2003, *ApJ*, 588, 18
- Gal-Yam, A., Mazzali, P., Ofek, E. O., Nugent, P. E., Kulkarni, S. R., Kasliwal, M. M., Quimby, R. M., Filippenko, A. V., Cenko, S. B., Chornock, R., Waldman, R., Kasen, D., Sullivan, M., Beshore, E. C., Drake, A. J., Thomas, R. C., Bloom, J. S., Poznanski, D., Miller, A. A., Foley, R. J., Silverman, J. M., Arcavi, I., Ellis, R. S., & Deng, J. 2009, *Nature*, 462, 624
- Galli, D. & Palla, F. 1998, *A&A*, 335, 403
- Greif, T. H. & Bromm, V. 2006, *MNRAS*, 373, 128
- Haiman, Z., Rees, M. J., & Loeb, A. 1997, *ApJ*, 476, 458
- Heger, A., Fryer, C. L., Woosley, S. E., Langer, N., & Hartmann, D. H. 2003, *ApJ*, 591, 288

- Heger, A. & Woosley, S. E. 2002, *ApJ*, 567, 532
- Hoffman, Y. & Ribak, E. 1991, *ApJ*, 380, L5
- Ivezić, Ž. et al 2008, *ApJ*, 684, 287
- Karlsson, T., Johnson, J. L., & Bromm, V. 2008, *ApJ*, 679, 6
- Komatsu, E., Dunkley, J., Nolta, M. R., Bennett, C. L., Gold, B., Hinshaw, G., Jarosik, N., Larson, D., Limon, M., Page, L., Spergel, D. N., Halpern, M., Hill, R. S., Kogut, A., Meyer, S. S., Tucker, G. S., Weiland, J. L., Wollack, E., & Wright, E. L. 2009, *ApJS*, 180, 330
- Komiya, Y., Habe, A., Suda, T., & Fujimoto, M. Y. 2009, *ApJ*, 696, L79
- Komiya, Y., Suda, T., Minaguchi, H., Shigeyama, T., Aoki, W., & Fujimoto, M. Y. 2007, *ApJ*, 658, 367
- Kroupa, P. 2002, *Science*, 295, 82
- Larson, R. B. 2005, *MNRAS*, 359, 211
- Lepp, S. & Shull, J. M. 1983, *ApJ*, 270, 578
- Lynden-Bell, D. 1967, *MNRAS*, 136, 101
- Machacek, M. E., Bryan, G. L., & Abel, T. 2003, *MNRAS*, 338, 273
- Madau, P., Ferrara, A., & Rees, M. J. 2001, *ApJ*, 555, 92
- Naoz, S., Noter, S., & Barkana, R. 2006, *MNRAS*, 373, L98
- Omukai, K., Tsuribe, T., Schneider, R., & Ferrara, A. 2005, *ApJ*, 626, 627
- O’Shea, B. W. & Norman, M. L. 2007, *ApJ*, 654, 66
- . 2008, *ApJ*, 673, 14
- Schaerer, D. 2003, *A&A*, 397, 527
- Salvadori, S., Schneider, R., & Ferrara, A. 2007, *MNRAS*, 381, 647
- Santoro, F. & Shull, J. M. 2006, *ApJ*, 643, 26
- Schneider, R., Omukai, K., Inoue, A. K., & Ferrara, A. 2006, *MNRAS*, 369, 1437

- Schörck, T., Christlieb, N., Cohen, J. G., Beers, T. C., Shectman, S., Thompson, I., McWilliam, A., Bessell, M. S., Norris, J. E., Meléndez, J., Ramírez, S., Haynes, D., Cass, P., Hartley, M., Russell, K., Watson, F., Zickgraf, F., Behnke, B., Fechner, C., Fuhrmeister, B., Barklem, P. S., Edvardsson, B., Frebel, A., Wisotzki, L., & Reimers, D. 2009, *A&A*, 507, 817
- Sheth, R. K. & Tormen, G. 1999, *MNRAS*, 308, 119
- Smith, B. D., Turk, M. J., Sigurdsson, S., O’Shea, B. W., & Norman, M. L. 2009, *ApJ*, 691, 441
- Tan, J. C. & McKee, C. F. 2004, *ApJ*, 603, 383
- Tegmark, M., Silk, J., Rees, M. J., Blanchard, A., Abel, T., & Palla, F. 1997, *ApJ*, 474, 1
- Trenti, M., Santos, M. R., & Stiavelli, M. 2008, *ApJ*, 687, 1
- Trenti, M. & Stiavelli, M. 2007, *ApJ*, 667, 38
- . 2009, *ApJ*, 694, 879
- Trenti, M., Stiavelli, M., & Shull, J. M. 2009, *ApJ*, 700, 1672
- Tumlinson, J. 2006, *ApJ*, 641, 1
- . 2007, *ApJ*, 664, L63
- . 2009, *ArXiv e-prints*
- Tumlinson, J., Venkatesan, A., & Shull, J. M. 2004, *ApJ*, 612, 602
- Weinmann, S. M. & Lilly, S. J. 2005, *ApJ*, 624, 526
- Yoshida, N., Abel, T., Hernquist, L., & Sugiyama, N. 2003, *ApJ*, 592, 645
- Yoshida, N., Omukai, K., Hernquist, L., & Abel, T. 2006, *ApJ*, 652, 6

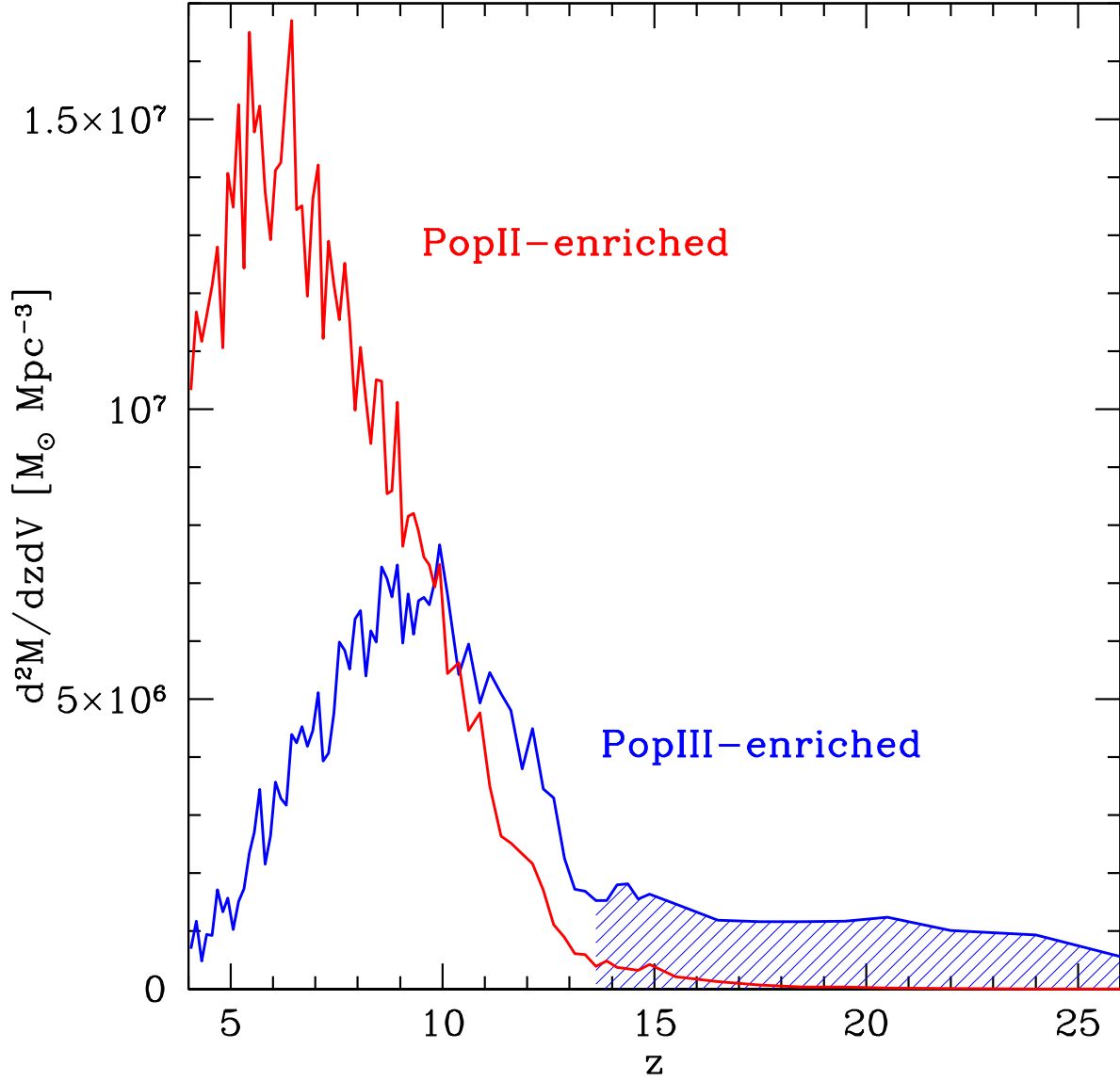


Fig. 1.— Formation rate per unit redshift of second-generation gas ($M_{\odot} \text{ Mpc}^{-3} dz^{-1}$) enriched to metallicity $Z \sim 10^{-3.5} Z_{\odot}$ as measured from a 10^3 Mpc^3 cosmological simulation that takes into account radiative feedback for Population III formation, self-enrichment of halos, and metal winds propagating at 60 km s^{-1} (see Trenti et al. 2009). The rate of gas enriched by Pop III stars is shown as a solid blue line, while the rate for Pop II-enriched gas is shown as solid red line. The blue shaded area represents the gas enriched by Population III stars formed in minihalos (cooled by H_2). Most second-generation stars in the volume are formed near the end of the reionization era, at redshifts $z \lesssim 10$.

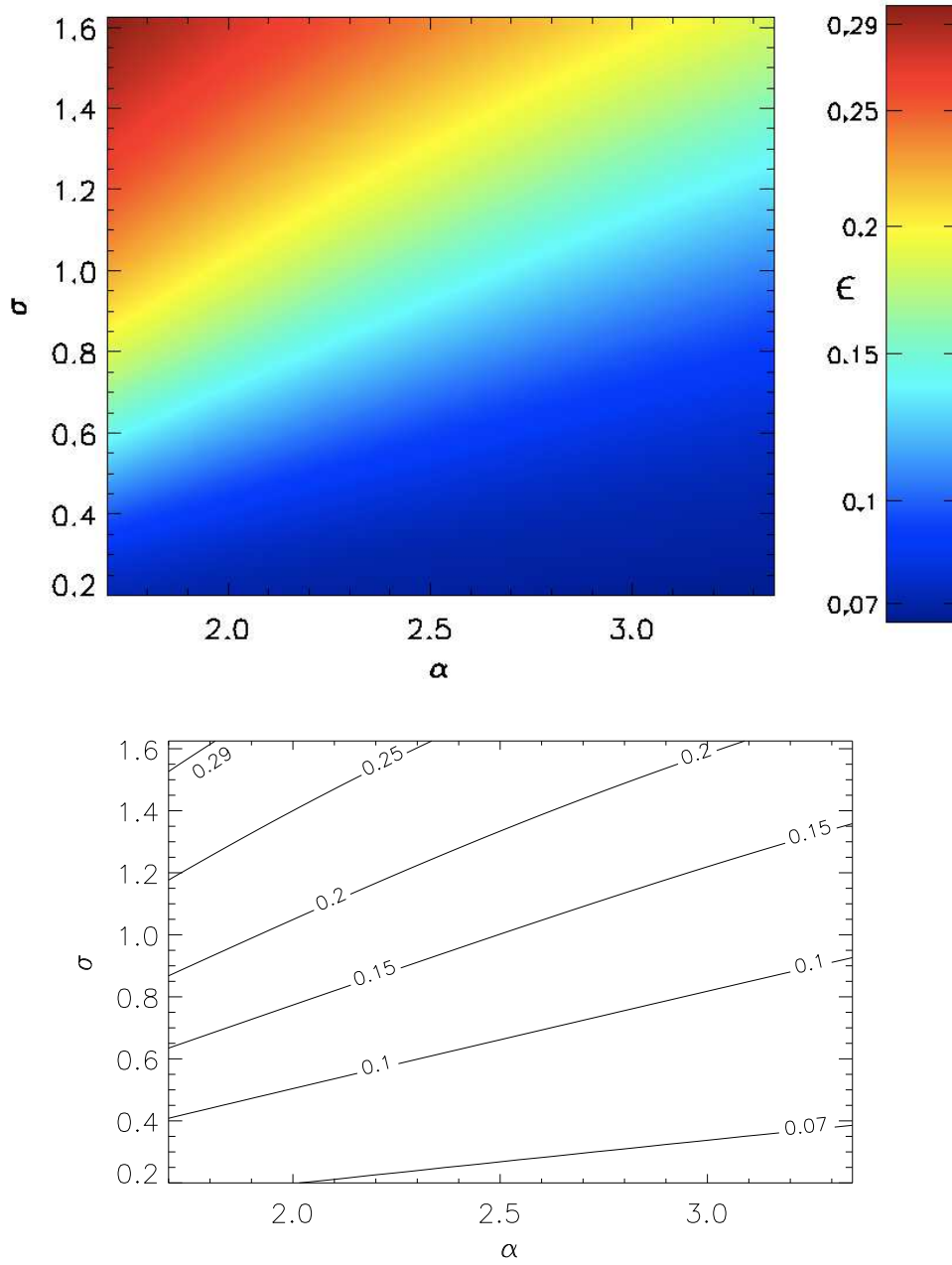


Fig. 2.— Upper panel: Image showing the ratio ϵ of stars enriched by Population III to total number of second-generation stars (with initial mass $M \leq 0.9 M_{\odot}$) on the main sequence or giant branch in the current universe, plotted as function of log-normal IMF parameters α and σ . Color coding for ϵ is given by the color bar on the right. Lower panel: contour lines for $\epsilon(\alpha, \sigma) = 0.07, 0.1, 0.15, 0.20, 0.25, 0.29$ (from bottom to top).

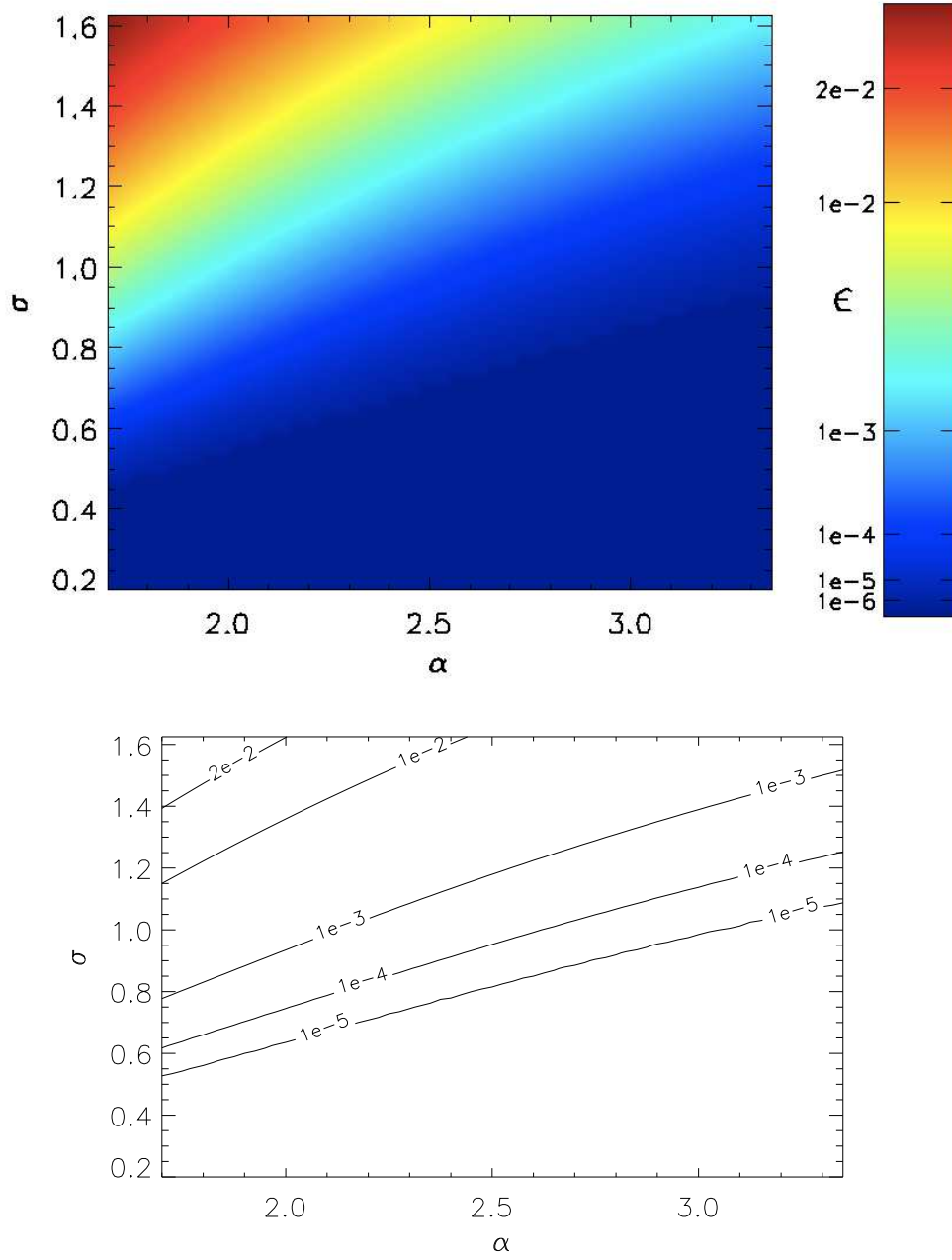


Fig. 3.— Same as Fig. 2, but considering only second-generation stars enriched by the Population III stars in minihalos. This second-generation gas is represented as shaded area in Fig. 1. Contour lines are for much smaller values of $\epsilon = 10^{-5}, 10^{-4}, 10^{-3}, 10^{-2}, 2 \times 10^{-2}$ from bottom to top. Studies of extremely metal-poor stars will need a very large sample to constrain the IMF of Population III stars progenitors in minihalos.

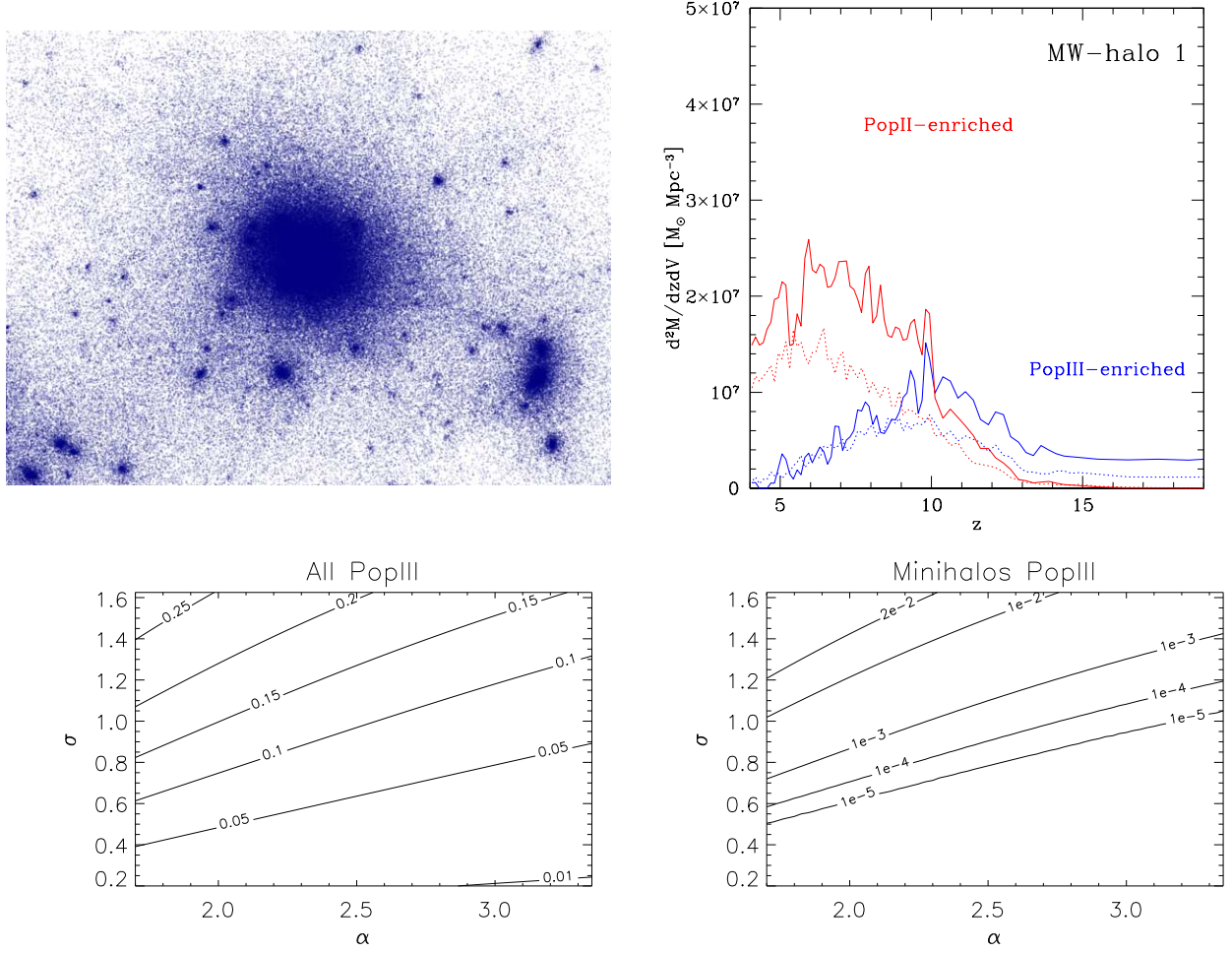


Fig. 4.— MW-like halo 1 ($M_1 = 3.15 \times 10^{12} M_\odot$ at $z = 0$). Upper left: halo projection at $z = 0$ (from the low-resolution run). The image size is $1.3 \times 0.97 \text{ Mpc}^2$. Upper right: formation rate of second-generation gas at high redshift within the comoving volume that ends up in the halo at $z = 0$ (solid lines). This panel is the equivalent of Fig. 1, obtained for $v_{wind} = 60 \text{ km s}^{-1}$. For comparison, dotted lines show the average formation rate of second-generation gas from Fig. 1. Smoothing over two data points has been applied for the solid lines. Bottom left panel: Contour lines for the ratio ϵ of stars enriched by Population III to total number of second-generation stars for halo 1. This panel is the equivalent of Fig. 2. Bottom right panel: like in bottom left panel, but considering only Population III stars in minihalos (equivalent to Fig. 3).

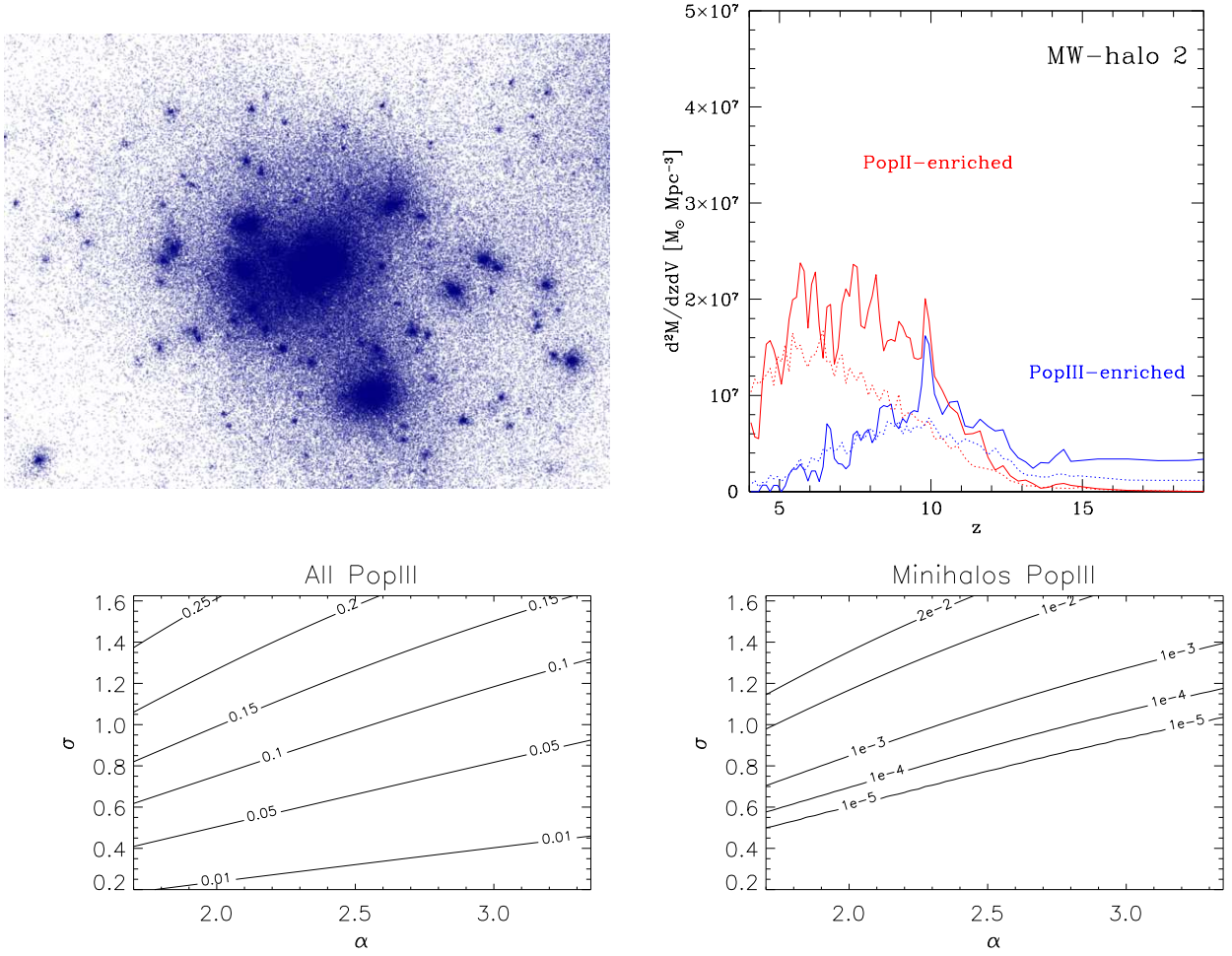


Fig. 5.— Same as Figure 4 for MW-like halo 2 ($M_2 = 2.60 \times 10^{12} M_\odot$ at $z = 0$).

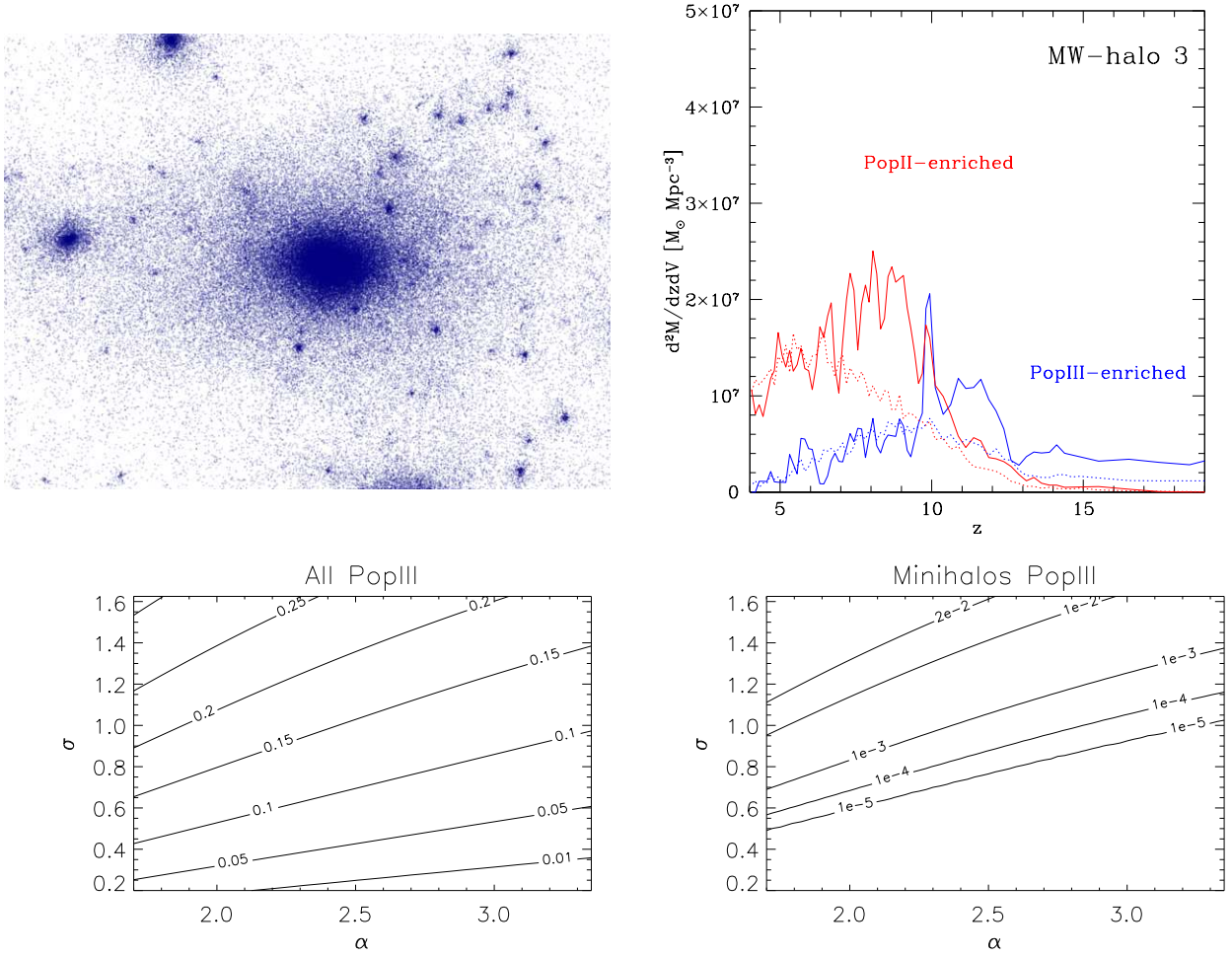


Fig. 6.— Same as Figure 4 for MW-like halo 3 ($M_2 = 1.59 \times 10^{12} M_\odot$ at $z = 0$).

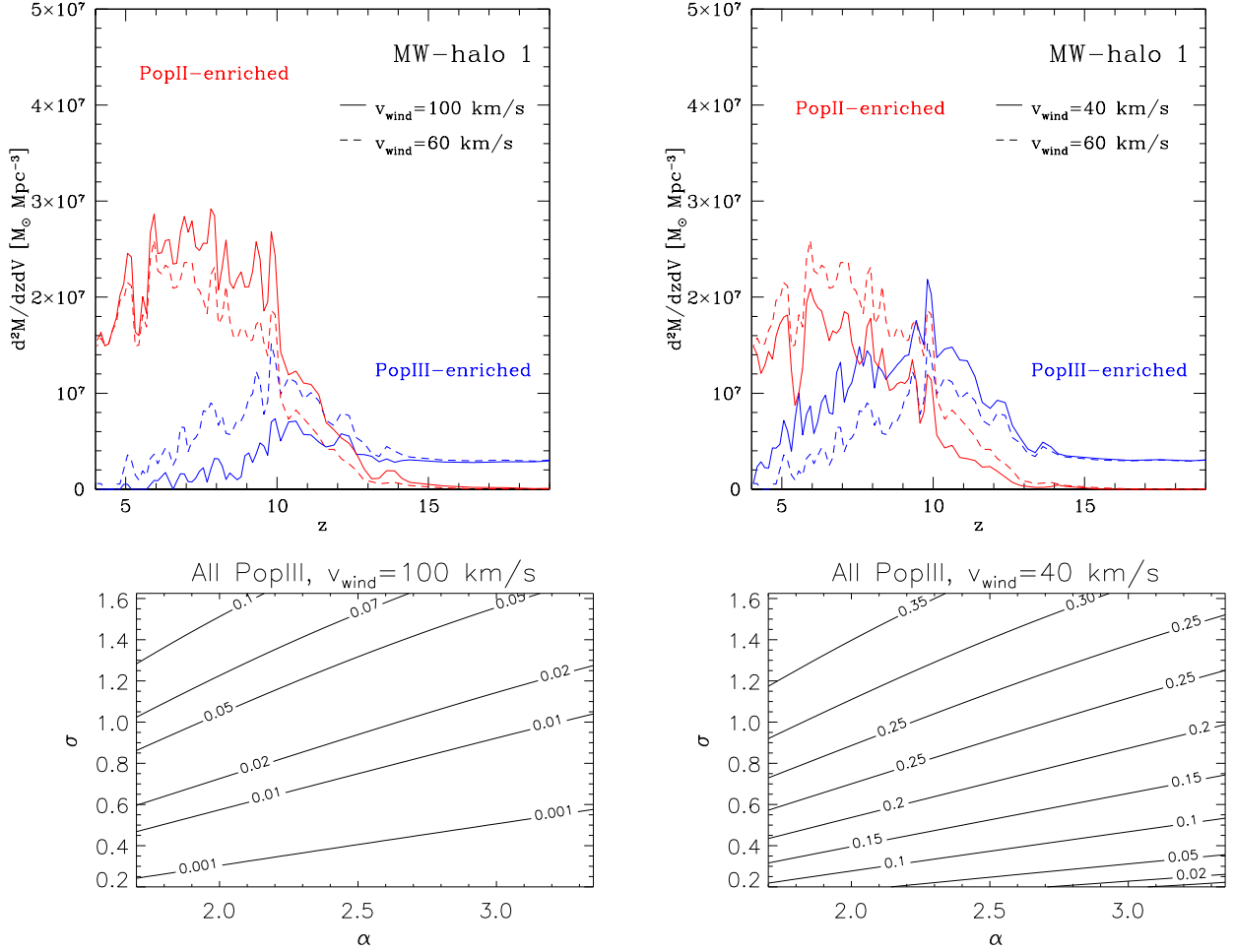


Fig. 7.— Influence of metal outflow speed on our modeling for MW-like halo 1 (see Figure 4). Left column shows results with $v_{wind} = 100 \text{ km s}^{-1}$, and right column shows $v_{wind} = 40 \text{ km s}^{-1}$. Upper panels (formation rate of second-generation gas) show for comparison our standard model, $v_{wind} = 60 \text{ km s}^{-1}$, as dashed lines. Bottom panels show contour lines for the ratio ϵ of stars enriched by Population III to total number of second-generation stars.

Table 1: Required sample size of EMP stars with $Z \leq 10^{-3.4} Z_{\odot}$

α	σ	$N_{min-AllPopIII}$		$N_{min-MinihalopopIII}$	
1.7	0.3	118	274	$> 10^7$	$> 10^7$
1.7	0.6	65	95	1.35×10^5	6.63×10^4
1.7	1.0	41	49	1775	1008
2.5	0.3	130	449	$> 10^7$	$> 10^7$
2.5	0.6	99	202	$> 10^7$	$> 10^7$
2.5	1.0	62	87	5.09×10^5	2.54×10^4
3.35	0.3	135	588	$> 10^7$	$> 10^7$
3.35	0.6	120	344	$> 10^7$	$> 10^7$
3.35	1.0	86	151	4.61×10^6	2.30×10^6

Note. — Minimum number (N_{min} , see Equation 6) of second-generation stars needed to rule out at a confidence level of 99% the hypothesis that a fraction 50% of Population III stars exploded as PISN (third column) as a function of the second-generation IMF parameters α and σ . The first value of N_{min} refers to the box average, the second value to MW-like halo 1. The last column reports the minimum number of second-generation stars needed to rule out, at the same confidence level, PISN in minihalos Population III stars. For some of the IMF parameter space, the number of stars needed exceeds 10^7 . The values of the characteristic IMF width σ reported here are those assumed in Tumlinson (2006).